J Neuropathol Exp Neurol
Vol. 73, No. 6
June 2014
pp. 536–547

ORIGINAL ARTICLE

Oligodendrocyte Loss During the Disease Course in a Canine Model of the Lysosomal Storage Disease Fucosidosis

Jessica L. Fletcher, BAnVetBioSc (Hons 1), PhD, Gauthami S. Kondagari, MVSc, PhD, Charles H. Vite, DVM, PhD, Peter Williamson, BSc (Hons), PhD, and Rosanne M. Taylor, BVSc (Hons 1), DipVetClinStud, PhD

Abstract

Hypomyelination is a poorly understood feature of many neurodegenerative lysosomal storage diseases, including fucosidosis in children and animals. To gain insight into hypomyelination in fucosidosis, we investigated lysosomal storage, oligodendrocyte death, and axonal and neuron loss in CNS tissues of fucosidosis-affected dogs aged 3 weeks to 42 months using immunohistochemistry, electron microscopy, and gene expression assays. Vacuole accumulation in fucosidosis oligodendrocytes commenced by 5 weeks of age; all oligodendrocytes were affected by 16 weeks. Despite progressive vacuolation, mature oligodendrocyte loss by apoptosis (caspase-6 positive) in the corpus callosum and cerebellar white matter stabilized by 16 weeks, with no further subsequent loss. Axonal neurofilament loss progressed only in late disease, suggesting that disturbed axon-oligodendrocyte interactions are unlikely to be the primary cause of hypomyelination. A 67% decline in the number of Purkinje cell layer oligodendrocytes coincided with a 67% increase in the number of caspase-6–positive Purkinje cells at 16 weeks, suggesting that early oligodendrocyte loss contributes to Purkinje cell apoptosis. Fucosidosis hypomyelination appeared to follow normal spatiotemporal patterns of myelination, with greater loss of oligodendrocytes and larger downregulation of *CNP*, *MAL*, and *PLP1* genes at 16 weeks in the cerebellum versus the frontal cortex. These studies suggest that survival of oligodendrocytes in fucosidosis is limited during active myelination, although the mechanisms remain unknown.

From the Faculty of Veterinary Science, The University of Sydney, Camperdown, New South Wales, Australia (JLF, GSK, PW, RMT); and Section of Medical Genetics, School of Veterinary Medicine, University of Pennsylvania, Philadelphia, Pennsylvania (CHV).

Send correspondence and reprint requests to: Rosanne M. Taylor, BVSc (Hons 1), DipVetClinStud, PhD, Faculty of Veterinary Science, The University of Sydney, Rm 204, JD Stewart Bldg (B01), Camperdown, NSW 2006, Australia; E-mail: rosanne.taylor@sydney.edu.au

The National Institutes of Health (Grant No. RR02512) supported the fucosidosis research colony maintained at the University of Pennsylvania by Professor Mark Haskins, from which PF1 and PF2 tissue samples were obtained. The remainder of this work was supported by bequests to the Faculty of Veterinary Science, The University of Sydney.

The authors declare that they have no conflicts of interest.

Supplemental digital content is available for this article. Direct URL citations appear in the printed text and are provided in the HTML and PDF versions of this article on the journal's Web site (www.jneuropath.com).

Key Words: Apoptosis, Fucosidosis, Hypomyelination, Lysosomal storage disease, Oligodendrocytes.

INTRODUCTION

Fucosidosis caused by deficiency in the lysosomal enzyme α-L-fucosidase is a progressive neurologic lysosomal storage disease (LSD). Central nervous system (CNS) myelin loss is an early pathologic feature of infantile-onset cases (1–4), and myelin abnormalities were identified by magnetic resonance imaging in the cerebellum and cerebrum of an 8-month-old child with fucosidosis (4). In canine fucosidosis, CNS myelin loss in the cerebellum and cerebrum is detectable from 8 weeks of age, many months before the first neurologic signs (5, 6). By 16 weeks, when clinical signs of anxiety and learning delays are inconsistent, myelin deficits are most severe in the earlier myelinating tracts of the cerebellum compared to the later maturing corpus callosum of the cerebrum. Fine proprioceptive deficits and poorly modulated postural adjustments possibly caused by neuron loss and conduction deficits from hypomyelination in large, fast-conducting sensory and motor tracts do not manifest in fucosidosis-affected dogs until considerably later (at 8–12 months of age) (5, 6). At this time, white matter tracts show dispersion of myelinated axons and infiltration of vacuolated macrophages, in addition to a 21% loss of myelin relative to age-matched controls (5). Myelin deficits in canine fucosidosis progress in advanced disease (aged ≥24 months) as widespread vacuolation displaces myelinated tracts and as macrophage infiltration and glial reactivity increase (5).

Hypomyelination is the failure of normal myelin deposition attributable to oligodendrocyte dysfunction during active postnatal myelination (3). Downregulation of oligodendrocytes and myelin-specific genes at 16 weeks in the frontal cerebrum of fucosidosis-affected pups (7) suggests that the 14% loss of corpus callosum myelin in fucosidosis at this time (5) (when cerebral white matter development in dogs is in progress [8, 9]) may be attributable to hypomyelination rather than to active myelin destruction. Reduced expression of *CNP*, *MAG*, *MAL*, *MRF*, and *OPALIN* genes, which code for proteins involved in oligodendrocyte differentiation, and myelin membrane elaboration suggest that α-L-fucosidase deficiency may directly impede

postnatal oligodendrocyte development and myelin deposition. Deficiency in α-L-fucosidase prevents the full maturation of other postnatally maturing cells, best exemplified by spermatozoa. These fail to mature and achieve full motility in canine fucosidosis because of failure to remove midpiece cellular remnants during the epididymal maturation process (10).

The cause of hypomyelination in fucosidosis is unclear because the roles of the lysosomal system in oligodendrocyte differentiation, metabolism, and myelin elaboration are not understood. Substrate toxicity, as seen in globoid cell leukodystrophy (11), is not consistent with the rate of myelin loss during disease progression (5, 12–14), the absence of myelin debris and lipid-containing macrophages (15–18), or the normal appearance of fucosidosis myelin sheaths in fucosidosis (17–19). Despite this, the rapid rise in cortical fucosyl-*N*-acetyl glucosaminyl aspartate from near-normal levels at birth to 3 times these levels in the cerebellum and cerebellum at 16 weeks (20) may impair oligodendrocyte metabolism. Oligodendrocytes are particularly vulnerable to cellular disturbance during elaboration of myelin sheaths owing to high metabolic requirements (21–23). In fucosidosis, progressive lysosomal enlargement within oligodendrocytes may result in activation of cathepsin-mediated lysosomal stress pathways and, ultimately, their apoptotic cell death (24). Fucosylated substrate accumulation within lysosomes may also have a direct effect on the synthesis or export of myelin components, causing reduced myelin deposition. Lysosomal exocytosis of the myelin structural protein proteolipid protein-1 (PLP1) to the plasma membrane is critical to the assembly of myelin sheaths (25), and the temporal expression of paranodal loop protein myelin-associated glycoprotein (MAG) isoforms regulated by lysosomal degradation (26) may also be affected. Evidence of either vacuolation or loss of oligodendrocytes has yet to be identified in human or canine fucosidosis despite histologic findings of reduced CNS myelin density in both terminal stages of human fucosidosis (16, 27) and all stages of canine fucosidosis (5, 17).

Neurotransmission along axons, synaptic release of adenosine, and downregulation of polysialylated neural cell adhesion molecules on the axon surface are required for oligodendrocytes to recognize and initiate plasma membrane extension around axons (28, 29). Disrupted axon-oligodendrocyte signaling caused by neuron dysfunction and axon dysmorphology may contribute to hypomyelination (1, 30–32). This mechanism of myelin loss has been proposed in murine Niemann-Pick type C disease model, an LSD in which axonal loss occurs before completion of postnatal myelination (at 9 days of age) (31, 33). In canine fucosidosis, neuronal pathology develops during active myelination; neuronal vacuolation is well established by 8 weeks, and axonal spheroids are present in cerebellar white matter from birth (34). These neuronal disturbances have the potential to disrupt axonal excitation during postnatal oligodendrocyte maturation, thereby limiting oligodendrocyte survival.

The present study investigates the effects of lysosomal disease on oligodendrocytes and axons in fucosidosis-affected dogs from 3 weeks to 42 months of age to gain insight into events associated with early fucosidosis myelin paucity. In particular, we aimed to characterize oligodendrocyte survival during canine postnatal myelination to determine whether axonal degeneration in early disease contributes to myelin loss in preclinical fucosidosis.

MATERIALS AND METHODS

Sample Collection

Neural tissues for histopathology, immunostaining, and electron microscopy (EM) were obtained from a tissue bank compiled (between 1979 and 2011) from clinical fucosidosis cases presented to The University of Sydney Veterinary Teaching Hospital and from research colony animals produced with animal ethics committee approval. A neurologic dysfunction score (out of 100) was assigned before death and was composed of 3 major components: motor deficits (out of 50), mental and behavioral signs (out of 30), and sensory and other signs (out of 20) (Table, Supplemental Digital Content 1, http://links.lww.com/NEN/A583). Assessment of the neurologic dysfunction score followed a standardized neurologic examination (35), which assessed all cranial nerves, reflexes, postural response, proprioception, gait, and sensory responses. Animals were placed in groups based on age and severity of clinical signs (Table 1).

To examine regional differences in oligodendrocyte and myelin gene expression, we conducted gene expression studies on the cerebrum and cerebellum of 16-week-old fucosidosis-affected (n = 3) and age-matched control (n = 3) English Springer spaniel pups. Samples collected at necropsy were snap-frozen and stored in liquid nitrogen before RNA extraction and complementary DNA synthesis. These animals had been in an intracisternal enzyme replacement therapy study as affected controls, where they received 150-μL infusions of PBS via the cisterna magna 3 times at monthly intervals from 8 to 16 weeks of age (20). No functional enzyme was ever administered to these animals, and they tolerated the infusion procedure without adverse reactions (20). These samples were also used for morphometry, immunostaining, and EM (Table 1).

All procedures were approved by the Animal Ethics Committees at The University of Sydney and other institutions and followed the Australian Code of Practice for the Care and Use of Animals for Scientific Purposes.

Immunohistochemistry

Formalin-fixed paraffin-embedded blocks of a frontal cerebral slice collected from the coronal sulcus and gyri of the rostral dorsolateral cerebrum and the dorsal vermis of the cerebellum of dogs indicated in Table 1 were sectioned at 4 μm thickness and placed on silane-coated slides. The following immunostains were used: anti–caspase-6 (CASP6; polyclonal rabbit anti-CASP6, 1:2000; Abcam, Cambridge, United Kingdom) for apoptosis (36); anti–2′,3′-cyclic nucleotide 3′-phosphodiesterase (CNPase; monoclonal mouse anti-CNPase, 1:400; Millipore, Temecula, CA) for terminal differentiation and mature oligodendrocytes (23); and anti–neurofilament light chain (NfL; mouse monoclonal anti-NfL, 1:50; DakoCytomation, Glostrup, Denmark) for axonal filaments (37). After deparaffinization and rehydration, sections underwent heat-induced antigen retrieval at pH 6 (Target Retrieval Solution, pH 6; DakoCytomation) before endoge-

TABLE 1. Experimental Groupings Based on Age and Severity of Clinical Signs

Dog	Age	NDS(/100)	CNPase	NfL	CASP6	Axon Diameter	Semithin Sections	EM
Control puppy (n = 3)								
CP1	16 weeks		+	+	+	+	+	Cervical spinal cord
CP2	16 weeks		+	+	+	+	+	Cervical spinal cord
CP2	16 weeks		+	+	+	+	+	Cervical spinal cord
Control adult (n = 11)								
CA1	12 months					+	+	
CA2	>12 months		+	+				
CA3	>12 months		+	+				
CA4	>12 months		+	+				
CA5	>12 months		+	+				
CA6	>12 months		+					
CA7	>12 months		+					
CA8	>12 months		+					
CA9	>12 months		+					
CA10	60 months		Cerebellum only			+	+	
CA11	36 months		+					
Preclinical fucosidosis (n = 10)								
PF1	3 weeks	—					Medulla only	Medulla
PF2	5 weeks	—					Medulla, cervical spinal cord	Medulla, cervical spinal cord
PF3	12 weeks	1	+	+	+			
PF4	12 weeks	1	+	+	+		+	Cervical spinal cord
PF5	16 weeks	2	+		+			
PF6	16 weeks	1	+	+	+	+	+	Cervical spinal cord
PF7	16 weeks	1	+	+	Cerebellum only	+	+	Cervical spinal cord
PF8	20 weeks	1	+		Cerebellum only			
PF9	24 weeks	1	+		+			
PF10	24 weeks	1	+		Cerebrum only		+	
Early fucosidosis (n = 7)								
EF1	8 months	1				+	+	
EF2	12 months	4	+	+				
EF3	12 months	—	+	+				
EF4	12 months	6				+	+	
EF5	13 months	4	Cerebrum only			+	+	
EF6	15 months	—	Cerebrum only	+				
EF7	16 months	—	+					
Late fucosidosis (n = 6)								
LF1*	24 months	37	Cerebellum only				+	
LF2	28 months	48	Cerebrum only	+		+	+	
LF3	30 months	48	Cerebellum only				+	
LF4	30 months	63	Cerebrum only	+				
LF5	36 months	68	Cerebellum only			+	+	
LF6	42 months	46	Cerebrum only			+		

Studies were performed based on the condition and availability of tissues.

*LF1 was included in the late fucosidosis group because the NDS was closer to the other late fucosidosis-affected affected animals and there were no other available tissue samples within this age range to comprise a midprogression group.

For CNPase, NfL, and CASP6, (+) indicates that both frontal cerebrum and cerebellum sections were used, unless otherwise stated. For axon diameter, (+) indicates that cervical spinal cord sections were examined and used for measurement of axon diameters. For semithin sections, (+) indicates that the cervical spinal cord, medulla, and frontal cerebrum were examined, unless otherwise stated.

CA, control adult; CP, control puppy; EF, early fucosidosis; LF, late fucosidosis; NDS, neurologic dysfunction score; PF, preclinical fucosidosis.

nous peroxidase activity was blocked with 3% H_2O_2 in Tris-buffered saline. Immunostaining for CNPase and NfL was performed with an automated staining system (Autostainer Plus; DakoCytomation) using an EnVision Flex Mini kit (DakoCytomation) for mouse antibodies. Caspase-6 staining was performed manually using a biotinylated donkey anti-rabbit IgG secondary antibody (1:800) and an avidin-biotin peroxidase complex (Vectastain ABC; Vector Laboratories,

Burlingame CA). Staining was visualized using 3,3′-diamenobenzidine substrate with hematoxylin counterstain. Apoptosis was also detected with the Apoptag Peroxidase In Situ kit (Apoptag TUNEL; Millipore) using in situ deoxynucleotide transferase-mediated dUTP nick-end labeling (TUNEL), as previously described (7, 34).

Electron Microscopy

Sections of the cervical spinal cord and medulla from 3 control and 5 fucosidosis-affected animals were examined by EM to identify morphologic changes in oligodendrocytes (Table 1). The cervical spinal cord was chosen because it demonstrates greater anatomic uniformity across animals, whereas the medulla was selected because it is myelinated at a similar developmental time as the spinal cord (9). Tissues were fixed in 2.5% glutaraldehyde, postfixed in 2% osmium tetroxide, and embedded in epoxy resin blocks. Semithin (0.5–1 μm) sections were collected on glass slides and stained with 1% toluidine blue. Additional semithin sections of the medulla, cerebellum, and cerebral white matter from some animals were also prepared (Table 1). A minimum of 3 fields of view in all semithin sections were examined using light microscopy at 1,000× magnification to identify oligodendrocytes based on criteria that included relatively small ovoid nuclei with clumped chromatin and abundant cytoplasm (38, 39). Small, very dense cells were identified as ''dark oligodendrocytes,'' which became more abundant with completion of myelination (39). Identified oligodendrocytes were inspected for vacuolation and for their relationships with myelinated axons, neurons, and microglia. Ultrathin (0.1 μm) sections of the cervical spinal cord and medulla were collected on 3 × 3 mm copper grids and stained with 2% uranyl acetate and lead citrate. Specimens were examined using a Phillips CM120 Biofilter transmission electron microscope, and images were collected using Digital Micrograph (Gatan Inc, Pleasanton, CA). At the EM level, oligodendrocytes were identified according to the following criteria: 1) electron-dense cytoplasm and nucleus with chromatin clumped around the rim of the nuclear membrane; 2) absence of cytoplasmic fibrils; 3) numerous microtubules in cell processes; and 4) well-developed endoplasmic reticulum with flattened cisternae (40). These were inspected for relationships to myelinated axons, neurons, and microglia; for evidence of unwrapping myelin, and for thin myelin sheaths (remyelination). Sectioning, poststaining, EM, and imaging were performed at the Adelaide Microscopy Centre (The University of Adelaide) and the Australian Centre for Microscopy and Microanalysis (The University of Sydney).

Image Analysis

Photomicrographs for image analysis were taken using a digital camera (Olympus DP-70; Olympus Australia Ltd, Sydney, Australia) attached to a light microscope (Olympus BX-51; Olympus Australia Ltd). Light micrographs and electron micrographs were processed and analyzed using Image J (National Institutes of Health, Bethesda, MD).

Oligodendrocyte Counts

To assess the numbers of mature oligodendrocytes, we performed manual counts on 10 to 15 fields of view of corpus callosum and cerebellar white matter from animals indicated in Table 1 at 1,000× magnification, with animal identity masked. Oligodendrocytes were identified as cell nuclei with CNPase-positive cytoplasmic staining. Counts were expressed as total number of oligodendrocytes per square millimeter of cerebral or cerebellar white matter. Oligodendrocyte numbers were also assessed in the Purkinje cell layer of the cerebellum, where counts were performed on 10 fields of view from animals at 400× magnification (Table 1).

Quantification of Positive CASP6 and NfL Staining

The percentage areas of positive CASP6 and NfL immunostaining were measured using automated threshold function. Images were preprocessed using the color deconvolution function in ImageJ for NfL; CASP6 images were converted into hue, saturation, and brightness color space before analysis. For both stains, 10 to 15 fields of view of stained sections from animals indicated in Table 1 were captured at 400× magnification, with animal identity obscured. Owing to the rapid and transient nature of apoptosis, only age-matched samples from preclinical fucosidosis-affected and control pups were used for CASP6 analysis (Table 1).

CASP6-Positive Purkinje Cell Counts

To assess the number of apoptotic Purkinje cells in preclinical disease, we performed manual counts of the number of CASP6-positive Purkinje cells on immunostained sections of dorsal cerebellar folia at 400× magnification, with sample identity obscured (Table 1). Each of the 15 fields of view contained the border of the molecular and granular cell layers; the lengths were estimated using the line tool in Image J. The total numbers of Purkinje cells and the numbers of CASP6-positive Purkinje cells were counted and expressed as the percentage of CASP6-positive Purkinje cells per 1,000 μm. The absence or presence of vacuolation in each Purkinje cell was recorded, but degenerate Purkinje cells and empty baskets were only noted but not included in the counts.

Axon Diameters in the Cervical Spinal Cord

Axonal diameters without myelin sheaths were measured to investigate the effects of fucosidosis on axon size and density (Methods, Supplemental Digital Content 2, http://links.lww.com/NEN/A584).

Gene Expression

Relative expression of myelin genes *CNP*, *MAG*, *MAL*, and *PLP1* between 16-week-old affected dogs and unaffected controls was determined using quantitative reverse transcription–polymerase chain reaction, with *GAPDH* and *PPIA* as internal controls. Oligonucleotide primers for *CNP*, *GAPDH*, *MAG*, *MAL*, *PLP1*, and *PPIA* (Table 2) were designed from the canine genome CanFam 2.0 (May 2005) annotated reference sequences obtained from GenBank using Primer3 (41). RNA from the frontal lobe and cerebellum of each dog was extracted using the RNeasy Lipid Tissue Mini kit (Qiagen, Germantown, MD), and complementary DNA was synthesized from 2 μg of total RNA using reverse transcription (SuperScript III; Life Technologies, Carlsbad, CA) and oligo(dT) primer (Life Technologies). Quantitative reverse transcription–polymerase chain reaction was performed using a Rotor-Gene 6000 (Qiagen)

TABLE 2. Primers for Quantitative Reverse Transcription–Polymerase Chain Reaction

Primer	GenBank Accession No.	Sequence (5′ to 3′)	Position (p)	Product Size, bp
CNP (+)	XM_844467	CCCAGCTCAAGGAGAAGAAC	p548–568	
CNP (−)		TCAGGAACCAGCCGAAGTAG	p656–637	108
GAPDH (+)	NM_001003142	GCCAAGAGGGTCATCATCTC	p340–359	
GAPDH (−)		GGGGCCGTCCACGGTCTTCT	p567–548	228
MAL (+)	NM_001003253	CGGACCTGCTCTTCATCTTC	p91–110	
MAL (−)		AACACAGACACAAACATCACCC	p205–184	115
PLP1 (+)	NM_001013834	CTGGCTGAGGGCTTCTACAC	p259–278	
PLP1 (−)		CAGCAGAGCAGGCAAACAC	p514–496	256
PPIA (+)	NR_036670	ATGGATGGCGAGCCTTTG	p11–28	
PPIA (−)		CTTTTCCCCGTAGATGGACTTG	p222–200	211
MAG (+)	XM_848694.2	TGCCCTCACGCAACGTGACC	p1539–1558	
MAG (−)		CCCAGTCGCCTCTCACTCTCAT	p1935–1914	397

Primers were designed using the canine genome CanFam 2.0 annotated reference sequences released in May 2005.
(+) Forward primer; (−) reverse primer.

under the following conditions: initial denaturation at 95°C for 5 minutes, followed by 35 cycles of 95°C for 30 seconds, 60°C for 60 seconds, and 72°C for 60 seconds in the presence of 2.5 mmol/L $MgCl_2$ for *MAG* or 1.5 mmol/L $MgCl_2$ for the remaining primers and 2 μM of SYTO®9 fluorescent dye (Life Technologies). Relative gene expression was calculated using the $2^{-\Delta\Delta Ct}$ method (42).

Statistical Analysis

Data were analyzed using a restriction maximal likelihood model in GenStat (version 11.1.01575; VSN International Ltd) to examine the effects of disease presence and severity on CNPase oligodendrocyte counts and NfL percentage staining quantification. For CASP6-positive Purkinje cell counts, the effects of disease presence were examined; for CASP6 percentage staining quantification and gene expression studies, the effects of disease presence and brain region were examined. A value of $p < 0.05$ was considered significant.

RESULTS

Clinical Summary

Neurologic dysfunction scores for the animals from which neural tissue was obtained, including previously reported cases, are presented in Table 1 (5, 19). Briefly, fucosidosis-affected dogs aged less than 8 months demonstrated variable and subtle behavioral changes (anxiety, delayed learning, and unwillingness to accept restraint) and were termed ''preclinical.'' No sensory or motor deficits were observed during this period. By 8 to 12 months, all dogs showed subtle repeated proprioceptive deficits in repositioning weight-bearing limbs, hyperextended posture, hypermetria, and delays in development of learned behaviors. Behavioral changes increased in severity by 12 to 14 months. During ''early'' disease, there was a progressive delay in the acquisition of learned and innate behaviors (e.g. poor mothering with failure to nurse pups) and motor system dysfunction with gait deficits, proprioceptive loss, and establishment of a wide base stance. From 15 to 23 months, ataxia and behavioral changes were more pronounced, with intermittent spontaneous and positional nystagmus, hypermetria, and dysmetria. In ''late'' disease (>24 months), motor deficits dominated, with hypermetric ataxia, poor balance, and severe proprioceptive losses. Late disease was characterized by severe mental decline, and late affected dogs became disoriented and disconnected from their environment. They demonstrated variable neurologic abnormalities (including circling, muscle tremors, dysphagia, regurgitation, and jaw champing, with frequent falling) and showed erratic and unpredictable behavior.

Oligodendrocytes Are Vacuolated in Fucosidosis-Affected Animals During Postnatal Myelin Development

Oligodendrocytes were identified by EM (Fig. 1; Figure, Supplemental Digital Content 3, http://links.lww.com/NEN/A585; Figure, Supplemental Digital Content 4, http://links.lww.com/NEN/A586) and in semithin sections (Figure, Supplemental Digital Content 5, http://links.lww.com/NEN/A587) by their dense cytoplasm and clumped nuclear chromatin. In the 3-week-old fucosidosis-affected medulla, no oligodendrocytes demonstrated storage vacuoles, although several neurons, astrocytes, microglia, and pericytes were extensively vacuolated (Figure, Supplemental Digital Content 5, http://links.lww.com/NEN/A587). By 5 weeks, 66.7% of oligodendrocytes identified by EM and 41.2% to 80.0% of oligodendrocytes identified in semithin sections of the cervical spinal cord were vacuolated. Electron microscopy examination revealed 1 to 8 cytoplasmic vacuoles per cell; each vacuole ranged from 0.15 to 3.9 μm in diameter (Fig. 1; Figure, Supplemental Digital Content 3, http://links.lww.com/NEN/A585). No abnormalities in other cytoplasmic organelles, such as endoplasmic reticulum, Golgi apparatus, or mitochondria, were observed. At 5 weeks, 66.7% to 75.0% of oligodendrocytes identified in semithin sections of fucosidosis-affected medullas were vacuolated.

In the 16-week fucosidosis-affected spinal cords, all oligodendrocytes identified by EM had cytoplasmic vacuoles with stippled contents (Fig. 1; Figure, Supplemental Digital Content 4, http://links.lww.com/NEN/A586). These were more numerous than those in the cervical spinal cord of the 5-week-old animal, with 3 to 17 vacuoles per cell ranging from 0.40 to 1.02 μm in diameter (Fig. 1). Oligodendrocytes with numerous vacuoles demonstrated a disrupted cell architecture with a distorted

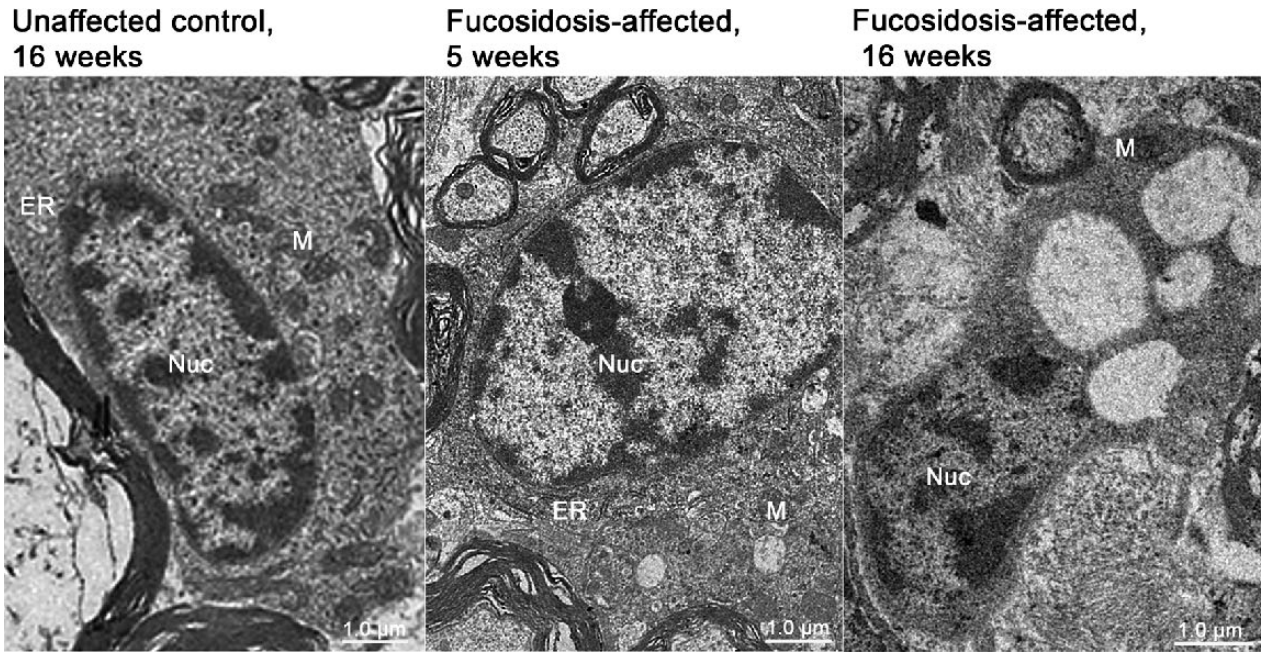

FIGURE 1. Electron photomicrographs of oligodendrocytes in the cervical spinal cord. Micrographs of cervical spinal cord oligodendrocytes from a 16-week-old unaffected control (2,800×), a 5-week-old fucosidosis-affected dog (2,800×), and a 16-week-old fucosidosis-affected dog (3,100×). ER, endoplasmic reticulum; M, mitochondria; Nuc, nucleus.

chromatin-dense nucleus (Fig. 1). Mitochondria, endoplasmic reticulum, and Golgi apparatus appeared normal. Vacuolated oligodendrocytes were also identified in semithin sections of the medulla, cerebellar white matter, and cerebral white matter (Figure, Supplemental Digital Content 5, http://links.lww.com/NEN/A587). In these regions and in the cervical spinal cord, vacuolated oligodendrocytes were closely associated with myelinated axons, although the cytoplasm was often distended (Figure, Supplemental Digital Content 5, http://links.lww.com/NEN/A587). Highly vacuolated astrocytes, microglia, and pericytes were dispersed throughout these white matter tracts (Figure, Supplemental Digital Content 5, http://links.lww.com/NEN/A587).

In the unaffected 16-week-old control dogs, a single 0.47 μm diameter vacuole was identified in 1 cervical spinal cord oligodendrocyte by EM. Vacuoles were not found in the remaining oligodendrocytes in unaffected dogs (Fig. 1).

Myelin sheaths in preclinical fucosidosis-affected dogs aged 3 to 16 weeks frequently appeared to be thin, ensheathing small axons, with only occasional thickly myelinated large axons (Figure, Supplemental Digital Content 3, http://links.lww.com/NEN/A585; Figure, Supplemental Digital Content 4, http://links.lww.com/NEN/A586). Similar findings were identified in unaffected controls (Figure, Supplemental Digital Content 4, http://links.lww.com/NEN/A586).

Oligodendrocytes Are Reduced in Fucosidosis-Affected Animals

In the cerebellar and cerebral white matter tracts of unaffected pups and adult dogs, CNPase staining was dark and intense, with oligodendrocytes identified by distinct cytoplasmic staining surrounding nuclei (Fig. 2, first row). The rich network of anti-CNPase immunostained oligodendrocyte processes surrounding the Purkinje cell baskets was markedly reduced to absent in all affected tissues compared with controls (Fig. 2, first row). Intense cytoplasmic CNPase staining was also observed in the cerebellar white matter tracts of all fucosidosis-affected animals regardless of age or disease progression. In the cerebral white matter tracts of fucosidosis-affected dogs, CNPase staining of processes was more diffuse than that in unaffected dogs (Fig. 2, second row).

There was a 1.8-fold decline in oligodendrocytes per square millimeter of cerebellar white matter in preclinical fucosidosis-affected dogs (497 ± 54) versus unaffected pups (907 ± 82) ($p < 0.001$). Oligodendrocytes per square millimeter of cerebellar white matter were also significantly decreased in early disease (443 ± 82) versus adult control dogs (717 ± 45) ($p < 0.001$). Late fucosidosis-affected dogs (643 ± 82) showed a trend toward a further decrease in oligodendrocytes per square millimeter of cerebellar white matter (Fig. 3a). No change in cerebellar oligodendrocyte numbers was detected with increasing disease severity or with normal aging.

The finding of pronounced reductions in the CNPase staining of the molecular and Purkinje cell layers of fucosidosis-affected cerebellum versus age-matched controls (Fig. 2) prompted us to investigate oligodendrocyte numbers in this region. Oligodendrocytes per millimeter length of Purkinje cell layer were significantly reduced in all stages of fucosidosis (preclinical, 7 ± 4; early, 10 ± 5; late, 8 ± 5) versus age-matched controls (pups, 21 ± 5; adults, 36 ± 3) ($p < 0.001$). There were also greater numbers of oligodendrocytes (1.7-fold increase) per millimeter of Purkinje cell layer in control adults versus pups, consistent with postnatal cerebellar development ($p < 0.001$) (Fig. 3b).

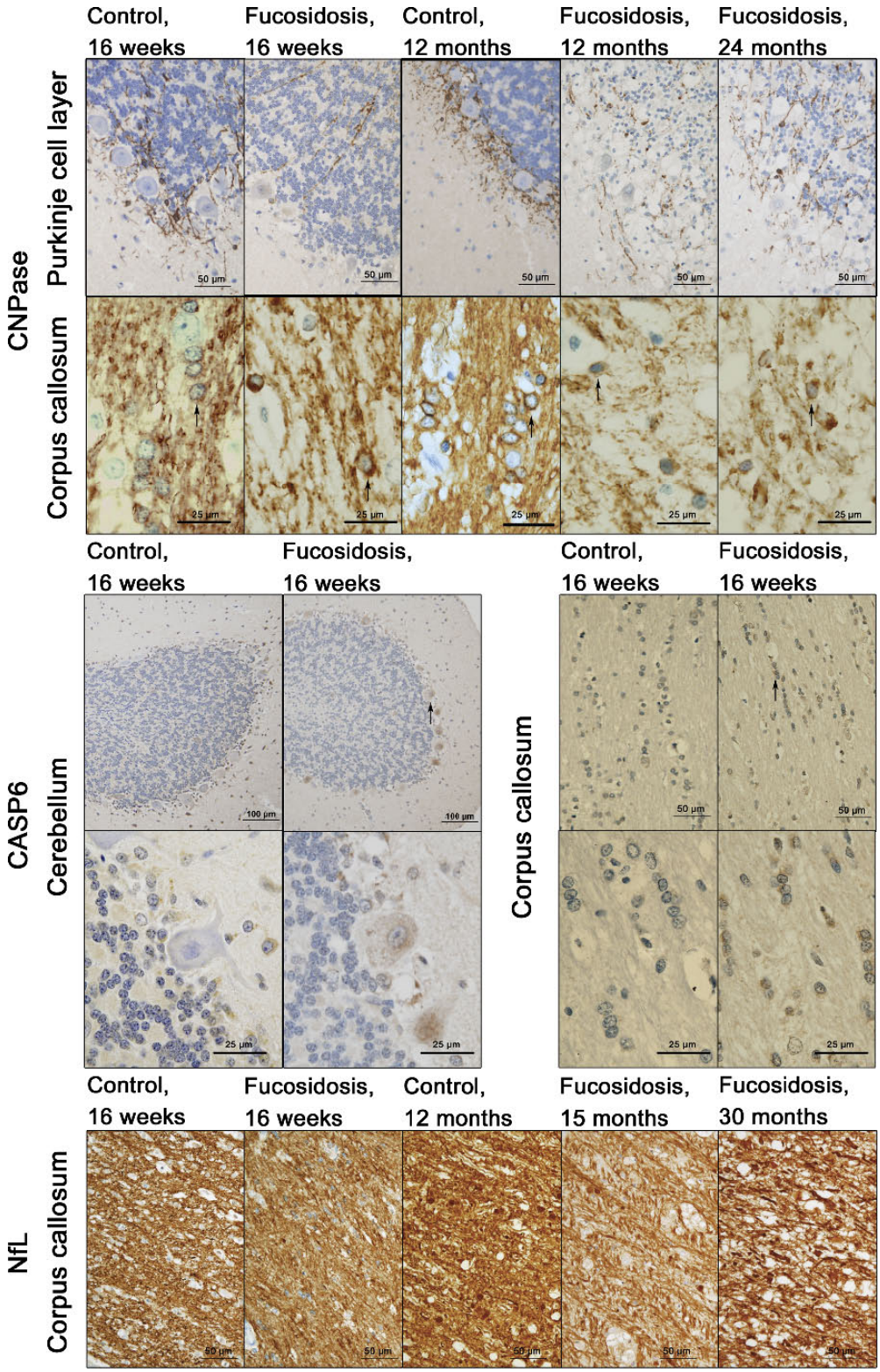

FIGURE 2. Immunostaining in the cerebellum and corpus callosum of control and fucosidosis-affected dogs at different ages. 2′,3′-Cyclic nucleotide 3′-phosphodiesterase staining in the Purkinje cell layer of the cerebellum and corpus callosum (top). Oligodendrocytes are indicated by arrows. Low- and high-magnification images of CASP6 immunostaining in the cerebellum and corpus callosum (middle). Caspase-6–positive cells are indicated by arrows. Neurofilament light chain immunostaining in the corpus callosum (bottom).

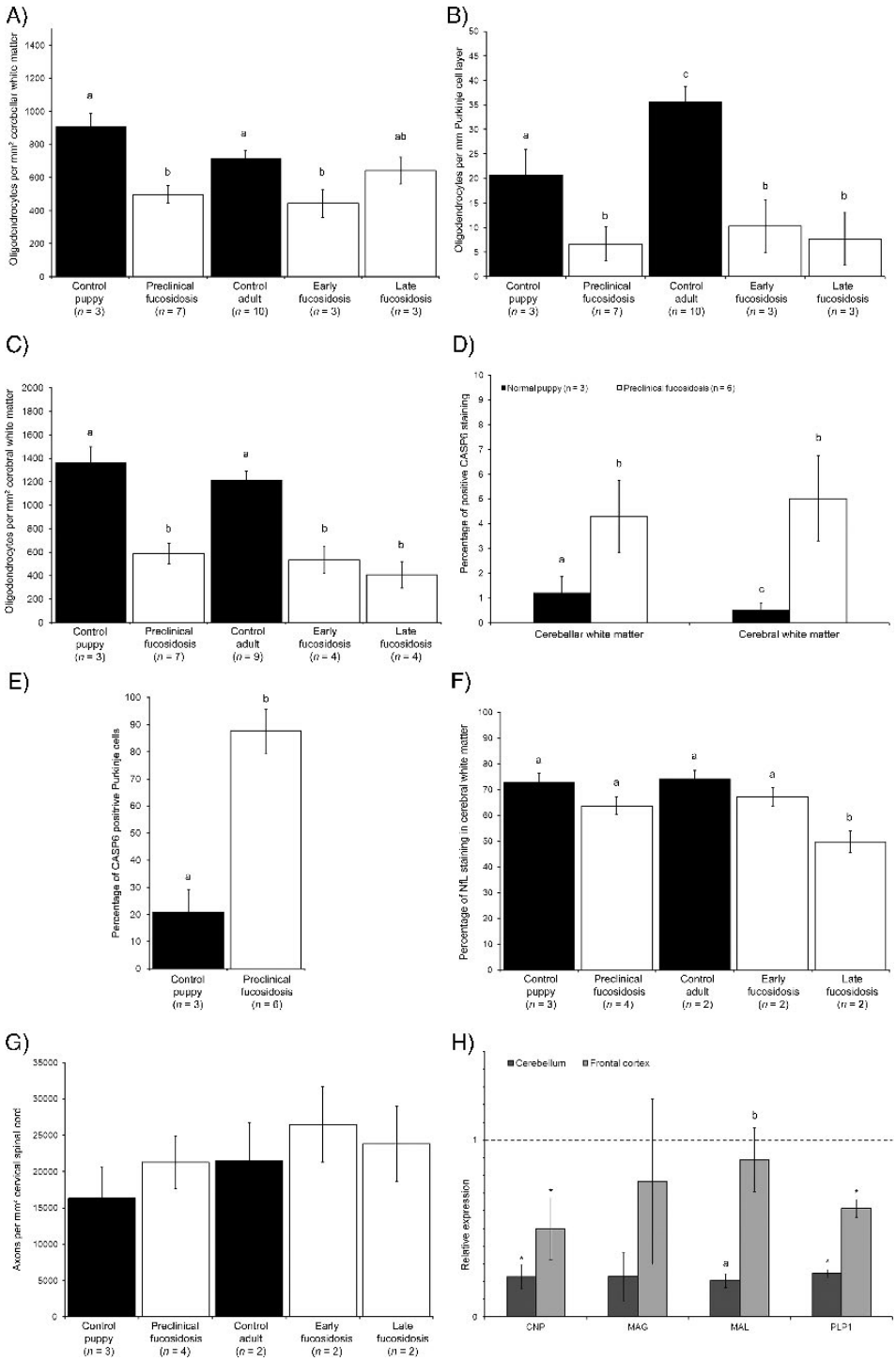

FIGURE 3. Oligodendrocyte loss, quantification of immunostaining, and relative gene expression. Oligodendrocyte counts in the cerebellar white matter **(A)**, Purkinje cell layer **(B)**, and corpus callosum **(C)** of normal age-matched controls (black) and preclinical, early, and late fucosidosis-affected dogs (white). Percentage of CASP6 staining in the cerebellar and cerebral white matter **(D)** and CASP6-positive Purkinje cells **(E)** in preclinical fucosidosis dogs (white) and age-matched controls (black). In cerebellar white matter, n = 7 for the preclinical fucosidosis group. Percentage of NfL immunostaining in the corpus callosum **(F)** of normal age-matched controls (black) and preclinical, early, and late fucosidosis-affected dogs (white). Axon density **(G)** as axons per square millimeter of the cervical spinal cord of age-matched controls (black) and preclinical, early, and late fucosidosis-affected dogs (white). Different letters (a–c) indicate significance ($p < 0.05$). Gene expression of *CNP*, *MAG*, *MAL*, and *PLP1* **(H)** in the cerebellum (black) and frontal cerebrum (gray) of fucosidosis-affected dogs relative to age-matched unaffected controls (1, dotted line). *Significantly different from controls. Different letters (a, b) indicate significant difference between regions in affected dogs ($p < 0.05$).

The number of oligodendrocytes per square millimeter of cerebral white matter was significantly reduced in preclinical (588 ± 86), early (558 ± 114), and late (407 ± 114) fucosidosis-affected dogs versus pups and adult age-matched controls (1,367 ± 131 and 1,215 ± 76, respectively) ($p < 0.001$) (Fig. 3c). In preclinical and early fucosidosis, this was a 2.3-fold decrease, whereas in fucosidosis-affected dogs older than 24 months, there was a 3.0-fold reduction. Comparison of preclinical, early, and late fucosidosis-affected dogs demonstrated no further significant loss in the number of oligodendrocytes with disease progression (Fig. 3c).

Apoptosis Increased in the White Matter and Purkinje Cell Layer of Preclinical Fucosidosis-Affected Animals

Diffuse CASP6 staining was observed in both cerebellar and cerebral white matter tracts of control pups, whereas darker staining was present in preclinical fucosidosis-affected pups (Fig. 2, middle, left). Positive cells in both normal and preclinical affected animals had diffuse halos of staining around cell nuclei that were small, irregular, and shrunken compared with those of CASP6-negative cells. Occasionally, darkly CASP6-positive nuclei were seen in preclinical fucosidosis-affected white matter. Chains of cells arranged linearly along white matter tracts, identified as putative oligodendrocytes, were occasionally immunopositive for CASP6 in both control and preclinical affected white matter tracts (Fig. 2, middle, right). This pattern of positive staining for apoptosis was also identified with Apoptag TUNEL staining (Figure, Supplemental Digital Content 6, http://links.lww.com/NEN/A588).

There was a significant 3.6- and 10.0-fold increase in the percentage of CASP6 staining in the cerebellar and cerebral white matter of preclinical fucosidosis-affected dogs (cerebellar, 4.3% ± 1.5%; cerebrocortical, 5.0% ± 1.7%) compared with that in unaffected pups (cerebellar, 1.2% ± 0.6%; cerebral, 0.5% ± 0.3%) ($p < 0.001$) (Fig. 3d). Caspase-6 staining in the cerebellar white matter of unaffected control pups was 2.4-fold higher than that in the cerebrocortical white matter of the same animals ($p < 0.001$) (Fig. 3d).

Caspase-6–positive Purkinje cells were significantly increased (by 66.7%) in preclinical fucosidosis-affected dogs versus age-matched controls, in which there were few CASP6-positive Purkinje cells ($p < 0.001$) (Fig. 3e). Caspase-6–positive Purkinje cells had granular cytoplasmic CASP6 staining (Fig. 2, middle, left); in preclinical fucosidosis-affected dogs, Purkinje cells occasionally had positive nuclear staining indicative of nuclear disassembly (Fig. 2, middle). Caspase-6–positive Bergmann glia were occasionally seen in preclinical affected dogs. All CASP6-positive Purkinje neurons in affected dogs showed cytoplasmic vacuolation (Fig. 2), whereas CASP6-positive neurons in controls were not vacuolated.

Axonal Changes

Axonal density in cerebral white matter was reduced in late fucosidosis. Neurofilament light chain staining in the cerebral white matter tracts of all dogs (both fucosidosis-affected and controls) was dark and intense, and the staining differed in clinically affected fucosidosis dog tissue because of prominent dispersion of stained axons by lysosomal vacuolation (Fig. 2, bottom; Figure, Supplemental Digital Content 7, http://links.lww.com/NEN/A589). Quantification revealed a 24.6% decrease in positive NfL staining in late fucosidosis-affected corpus callosum compared with unaffected adults ($p = 0.009$) (Fig. 3f). There was also a significant 13.8% to 17.4% decrease in NfL staining in late fucosidosis-affected versus preclinical and early fucosidosis-affected corpus callosum. No differences between the percentage of NfL-immunostained tissue in the corpus callosum of preclinical fucosidosis-affected and control pups, early fucosidosis-affected and unaffected adults, or preclinical and early fucosidosis-affected animals were detected (Fig. 3f). Axonal densities in the cervical spinal cord were not different at any stage of fucosidosis compared with unaffected age-matched controls ($p = 0.640$) (Fig. 3g).

Axon Diameters

The mean naked axon diameters in the corticospinal and spinocerebellar tracts of the cervical spinal cord were not different among fucosidosis-affected dogs at every stage of disease versus controls ($p = 0.431$) (Results, Supplemental Digital Content 2, http://links.lww.com/NEN/A584; Figure, Supplemental Digital Content 8, http://links.lww.com/NEN/A590).

Myelin Gene Expression

Myelin genes *CNP*, *MAG*, *MAL*, and *PLP1* were downregulated in 16-week-old fucosidosis-affected animals versus age-matched controls, with consistently greater downregulation in the fucosidosis-affected cerebellum versus the cerebrum (Fig. 3h). Relative *CNP* expression was reduced by 4.0-fold in the cerebellum and by 1.6-fold in the frontal lobe of affected dogs versus controls ($p = 0.013$). No differences between these brain regions were detected in affected animals. Relative *MAL* expression was reduced by 4.1-fold in fucosidosis-affected versus unaffected cerebrum ($p < 0.001$). There was also a 4.8-fold decrease in cerebellar *MAL* expression in affected dogs compared with controls ($p < 0.001$), but cerebral *MAL* expression was not different. Relative *PLP1* expression was reduced by 4.4-fold in the cerebellum and by 2.0-fold in the frontal cerebrum of fucosidosis-affected dogs versus controls ($p = 0.032$). No regional differences in *PLP1* expression were detected in affected or control dogs. Relative *MAG* expression in either the cerebellum or the cerebrum of affected dogs did not differ from that in age-matched controls ($p = 0.250$).

DISCUSSION

This is the first detailed study of oligodendrocyte and myelin abnormalities in canine fucosidosis. We document a time course of pathophysiology that first affects myelin formation through vacuolation, apoptotic oligodendrocyte loss, and consequent reduced expression of myelin-related genes before axon density declines in advanced clinical disease. Oligodendrocytes of the earlier myelinating cerebellum are the most affected, with severe loss in both Luxol fast blue–stained myelin (5) and Purkinje cell layer oligodendrocyte numbers. The severity of these cellular changes in the cerebellum is also reflected in the more substantial reductions in myelin gene expression in this region versus the frontal cerebrum. The

timing of oligodendrocyte loss in both the cerebrum and cerebellum coincides with increased numbers of Purkinje cells and cortical pyramidal neruons (34) vulnerable to apoptosis. In addition to myelination, oligodendrocytes provide reciprocal support to neurons, including the production of neuroprotective trophic insulin-like growth factor-1 and glial cell line–derived neurotrophic factor (43–47). Neuron death in fucosidosis is usually attributed to lysosomal vacuolation and neuroinflammation, with little consideration of a role for oligodendrocyte loss (5, 34). Here, we demonstrated that, in fucosidosis-affected dogs, Purkinje cells seem to be 4 times more vulnerable to apoptosis at 16 weeks of age, when Purkinje cell layer oligodendrocytes are markedly reduced. Remaining Purkinje cell numbers seem to be maintained until 8 to 10 months of age (when hypermetria and ataxia commence), but they demonstrate a significant progressive loss as clinical severity increases (34). We propose that this progressive loss, which is associated with increasing vacuolation and microglial activity (5, 34), is amplified by the early loss of supporting oligodendrocytes.

Oligodendrocyte populations and myelin gene expression are more severely affected in the cerebellum than in the corpus callosum; these temporal and regional changes correspond to anatomic patterns of brain and myelin development. The cerebellum develops early, with myelination in the canine brainstem and cerebellum completed at 5 to 6 weeks of age (9). Levels of fucosylated substrate in the cerebellum are similar to those in the cerebrum in preclinical fucosidosis (20). However, lesions are more severe, with 14% greater loss of Luxol fast blue–stained cerebellar myelin (5); a more extreme 4.0- to 4.8-fold decrease in cerebellar *CNP*, *MAL*, and *PLP1* gene expression compared with the frontal cerebrum; and a marked 3.1-fold decrease in Purkinje cell satellite oligodendrocytes at 16 weeks. This suggests that the severity of myelin loss in fucosidosis is not driven solely by levels of substrate accumulation and that the disease processes are also related to developmental events.

The canine corpus callosum actively myelinates at 16 weeks. Apoptotic oligodendrocytes are expected during this time, as demonstrated by 0.5% of CASP6 staining in unaffected age-matched controls. The 10-fold increase in CASP6 staining found in the corpus callosum of fucosidosis-affected dogs indicates that the disease increases the vulnerability of maturing oligodendrocytes to apoptosis and that this accounts for the significant loss of mature oligodendrocytes at 16 to 24 weeks. Intriguingly, cerebellar white matter, Purkinje cell layer, and corpus callosum oligodendrocyte populations remained stable during disease progression, with no further significant disease through early or advanced clinical disease. There was no recovery of oligodendrocytes in early or late disease. This may indicate that adult oligodendrocyte progenitor cells, also known as NG2-positive cells (48), are not activated by myelin loss in fucosidosis. Remyelination was difficult to identify because thin myelin sheaths were observed in both fucosidosis-affected and control dogs. Activation of adult oligodendrocyte progenitor cells and remyelination in fucosidosis should be established. It was not examined here owing to low species cross-reactivity levels of anti-NG2 antibodies among human, murine, and canine species, as well as poor results achieved on formalin-fixed paraffin-embedded tissues (which was the only sample type available) across species (48). Possible inert adult oligodendrocyte progenitor cells and stabilization of oligodendrocyte numbers after 16 weeks suggest that oligodendrocytes are exquisitely vulnerable to lysosomal enzyme–related impairment during maturation. This is consistent with the idea that oligodendrocyte survival through myelination is directly limited by the lysosomal defect in canine fucosidosis.

To test whether oligodendrocyte apoptosis is secondary to loss of axon-oligodendrocyte signaling during development (7), we considered axonal and oligodendrocyte markers throughout disease progression. There was no significant reduction in axon density in the corpus callosum or spinal cord, nor were there significant changes in axon diameter in affected preclinical dogs aged 12 to 32 weeks or in dogs showing early clinical signs at 8 to 15 months despite a significant decline in callosal and cerebellar oligodendrocyte population densities by 12 to 32 weeks. Axonal degeneration was only significant in the corpus callosum of severely affected dogs older than 24 months, when the rate of neuronal apoptosis increased 2.0-fold and 10% of pyramidal neurons in the frontal cortex were lost (34). From this, axon loss follows but does not drive early oligodendrocyte losses in canine fucosidosis. Instead, the 38% loss of myelin (5) and axonal degeneration characterized in advanced disease are proposed to be late effects that follow extensive damage by lysosomal engorgement and vacuolation in neurons, glial activation, and axonal dystrophy (5, 34).

Oligodendrocytes are highly metabolically active cells that produce and assemble myelin sheath lipids and proteins not only during active myelin development but also throughout life (26, 43, 49, 50). As such, vulnerability of oligodendrocytes to cellular disturbances is not unexpected. Lysosomal dysfunction, including the mild vacuolation of oligodendrocytes in the actively myelinating 5-week-old fucosidosis-affected medulla, may be sufficient to compromise oligodendrocyte function, resulting in hypomyelination. Direct insult to oligodendrocytes by substrate accumulation within lysosomes during preclinical fucosidosis would disrupt intracellular traffic involved in myelin synthesis. Because the major CNS myelin structural protein PLP1 is exported to the oligodendroglial plasma membrane through the lysosomal system, lysosomal engorgement would reduce the efficiency of myelin assembly (25). If this were the case, poorly compacted myelin with abnormal paranodal loops similar to the PLP1 mutant ''shaking pup'' (51) would also be expected; however, myelin sheaths in the spinal cord and medulla of fucosidosis-affected dogs appear morphologically normal from 3 weeks to 42 months of age, consistent with findings in the peripheral nervous system of fucosidosis-affected does in which myelin sheaths appear normal despite extensive Schwann cell vacuolation (18, 19).

More likely, vacuolation incites apoptotic cellular stress responses in maturing oligodendrocytes, as suggested by the increased CASP6 immunostaining of putative oligodendrocytes in the cerebellar white matter and corpus callosum at 16 weeks. Caspase-6 is an ''executioner'' caspase that interacts with additional executioners (i.e. caspase-2, caspase-3, and caspase-8) and is involved in the disassembly of the nuclear envelope during apoptosis (52). This premise of cellular stress induced

by lysosomal dysfunction resulting in apoptosis is broadly applicable to all cell types that demonstrate vacuolation in fucosidosis. It merits further investigation, through in vitro studies on cultured oligodendrocytes from fucosidosis-affected individuals, to identify the specific pathways involved.

The contribution of oligodendrocyte loss to neuronal apoptosis is rarely considered, but more than 22 LSDs have been shown to have myelin abnormalities (1); moreover, decreased myelin gene expression has been reported in mucopolysaccharidosis type VII, an LSD in which myelin loss is not a pathologic hallmark (53). In fucosidosis, a 3.1- to 4.6-fold loss of Purkinje cell satellite oligodendrocytes was consistently identified throughout the disease course, coinciding with a 4-fold increased vulnerability of Purkinje cells to apoptosis at 16 weeks and a comparable loss of Purkinje cells by 24 months (34). Because each CASP6-positive Purkinje neuron identified in preclinical fucosidosis dogs demonstrated extensive vacuolation, lysosomal enlargement must contribute to Purkinje cell apoptosis. Loss of trophic support provided by oligodendrocyte sodium channel clusters and production of growth factors (23, 43, 47) may increase the susceptibility of these large inhibitory neurons to cell death. Indeed, Purkinje cells and other GABAergic inhibitory neurons are known to have particular vulnerability to axonal dystrophy and loss in fucosidosis (34). In addition to the high metabolic requirements of these neuron types, loss of supporting oligodendrocytes and Bergmann glia (which were occasionally CASP6-positive in fucosidosis) may contribute to this vulnerability. Selective Purkinje cell loss is consistent with the onset and predominance of cerebellar motor deficits compared with the subtle proprioceptive deficits (which are indicative of cortical sensorimotor dysfunction) and cognitive impairment in 10- to 12-month-old dogs with fucosidosis.

Apoptotic oligodendrocyte loss in the cerebellum and corpus callosum at 16 weeks indicates that hypomyelination in canine fucosidosis is caused by limited oligodendrocyte survival during development. The reason for this is unclear. Impaired axon-oligodendrocyte signaling caused by axonal degeneration during active myelination can be eliminated because this is not significant until there is advanced disease. Disturbed myelin synthesis and export are less plausible because no structural myelin abnormalities are present in fucosidosis during the course of disease. Cellular stress response during oligodendrocyte maturation caused by α-L-fucosidase deficiency and vacuole accumulation is a possible cause that should be explored. Finally, the secondary role of oligodendrocytes in providing trophic support cells for neurons is likely important, and the initial and sustained decline of oligodendrocytes in fucosidosis may contribute to the vulnerability of Purkinje cells to apoptosis and clinical dysfunction in advancing canine fucosidosis.

ACKNOWLEDGMENTS

We thank Elaine Chew and Karen Barnes (Veterinary Pathology Diagnostic Service, The University of Sydney) and Associate Professor Peter Thomson for his advice on statistical analyses. We acknowledge the facilities and scientific/technical assistance of the Australian Microscopy and Microanalysis Research Facility at the Australian Centre for Microscopy and Microanalysis, The University of Adelaide, and The University of Sydney. We are also grateful to Professor Mark Haskins for maintaining the fucosidosis research colony at the University of Pennsylvania from which PF1 and PF2 tissue samples were obtained.

REFERENCES

1. Folkerth RD. Abnormalities of developing white matter in lysosomal storage diseases. J Neuropathol Exp Neurol 1999;58:887–902
2. Prietsch V, Arnold S, Kraegeloh-Mann I, et al. Severe hypomyelination as the leading neuroradiological sign in a patient with fucosidosis. Neuropediatrics 2008;39:51–54
3. Steenweg ME, Vanderver A, Blaser S, et al. Magnetic resonance imaging pattern recognition in hypomyelinating disorders. Brain 2010;133:2971–82
4. Vellodi A, Cragg H, Winchester B, et al. Allogenic bone marrow transplantation in fucosidosis. Bone Marrow Transplant 1995;15:153–58
5. Kondagari GS, Ramanthan P, Taylor RM. Canine fucosidosis: A neuroprogressive disorder. Neurodegener Dis 2011;8:240–51
6. Taylor RM, Farrow BRH, Healy PJ. Canine fucosidosis: Clinical findings. J Small Anim Pract 1987;28:291–300
7. Fletcher JL, Kondagari GS, Wright AL, et al. Myelin genes are downregulated in canine fucosidosis. Biochim Biophys Acta 2011;1812:1418–26
8. Miot-Noirault E, Barantin L, Akoka S, et al. T2 relaxation time as a marker of brain myelination: Experimental MR study in two neonatal animal models. J Neurosci Methods 1997;72:5–14
9. Gross B, Garcia-Tapia D, Riedesel E, et al. Normal canine brain maturation at magnetic resonance imaging. Vet Radiol Ultrasound 2010;51:361–73
10. Taylor RM, Martin IC, Farrow BRH. Reproductive abnormalities in canine fucosidosis. J Comp Pathol 1989;100:369–80
11. Suzuki K. Globoid cell leukodystrophy (Krabbe's disease): Update. J Child Neurol 2003;18:595–603
12. Fletcher JL, Williamson P, Horan D, et al. Clinical signs and neuropathologic abnormalities in working Australian Kelpies with globoid cell leukodystrophy (Krabbe disease). J Am Vet Med Assoc 2010;237:682–88
13. Gieselmann V. Metachromatic leukodystrophy: Genetics, pathogenesis and therapeutic options. Acta Paediatr 2008;97:15–21
14. Groeschel S, Kehrer C, Engel C, et al. Metachromatic leukodystrophy: Natural course of cerebral MRI changes in relation to clinical course. J Inherit Metab Dis 2011;34:1095–102
15. Alroy J, Ucci AA, Warren CD. Human and canine fucosidosis: A comparative lectin histochemistry study. Acta Neuropathol 1985;67:265–71
16. Durand P, Borrone C, Della Cella G. Fucosidosis. J Pediatr 1969;75:665–74
17. Hartley WJ, Canfield PJ, Donnelly TM. A suspected new canine storage disease. Acta Neuropathol 1982;56:225–32
18. Kelly WR, Clague AE, Barnes RJ, et al. Canine α-l-fucosidosis: A storage disease of Springer spaniels. Acta Neuropathol 1983;60:9–13
19. Taylor RM. *Canine Fucosidosis* [PhD thesis]. Sydney, Australia: The University of Sydney; 1988
20. Kondagari GS, King BM, Thomson PC, et al. Treatment of canine fucosidosis by intracisternal enzyme infusion. Exp Neurol 2011;230:218–26
21. Chrast R, Saher G, Nave K-M, et al. Lipid metabolism in myelinating glial cells: Lessons from human inherited disorders and mouse models. J Lipid Res 2010;52:419–34
22. Bradl M, Lassmann H. Oligodendrocytes: Biology and pathology. Acta Neuropathol 2010;119:37–53
23. de Castro F, Bribián A. The molecular orchestra of the migration of oligodendrocyte precursors during development. Brain Res Brain Res Rev 2005;49:227–41
24. Yamashima T, Oikawa S. The role of lysosomal rupture in neuronal death. Prog Neurobiol 2009;89:343–58
25. Trajkovic K, Dhaunchak AS, Goncalves JT, et al. Neuron to glia signalling triggers myelin membrane exocytosis from endosomal strorage sites. J Cell Biol 2006;172:937–48
26. Trapp BD, Pfeiffer SE, Anitei M, et al. Cell biology of myelin assembly. In: Lazzarini RA, ed. *Myelin Biology and Disorders*. San Diego, CA: Elsevier Academic Press, 2004:29–55
27. Willems PJ, Gatti R, Darby JK, et al. Fucosidosis revisited: A review of 77 patients. Am J Med Genet 1991;38:111–31
28. Barres BA, Raff MC. Proliferation of oligodendrocyte precursor cells depends on electrical activity in axons. Nature 1993;361:258–60

29. Coman I, Barbin G, Charles P, et al. Axonal signals in central nervous system myelination, demyelination and remyelination. J Neurol Sci 2005; 233:67–71
30. Ledesma MD, Prinetti A, Sonnino S, et al. Brain pathology in Niemann Pick disease type A: Insights from the acid sphingomyelinase knockout mice. J Neurochem 2011;116:779–88
31. Takikita S, Fukuda T, Mohri I, et al. Perturbed myelination process of premyelinating oligodendrocyte in Niemann-Pick type C mouse. J Neuropathol Exp Neurol 2004;63:660–73
32. Walkley SU, Sikora J, Miscenyi M, et al. Lysosomal compromise and brain dysfunction: Examining the role of neuroaxonal dystrophy. Biochem Soc Trans 2010;38:1436–41
33. Ong W-Y, Kumar U, Switzer RC, et al. Neurodegeneration in Niemann-Pick type C disease mice. Exp Brain Res 2001;141:218–31
34. Kondagari GS, Yang J, Taylor RM. Investigation of cerebrocortical and cerebellar pathology in canine fucosidosis and comparison to aged brain. Neurobiol Dis 2011;41:605–13
35. de Lahunta A, Glass E. Chapter 20: Neurologic exam. In: de Lahunta A, Glass E, Kent M, eds. *Veterinary Neuroanatomy and Clinical Neurology (Third Edition)*. St Louis, MO: Saunders Elsevier, 2009
36. Krajewska M, Rosenthal RE, Mikolajczyk J, et al. Early processing of Bid and capase-6, -8, -10, -14 in the canine brain during cardiac arrest and resuscitation. Exp Neurol 2004;189:261–79
37. Petzold A. Neurofilament phosphoforms: Surrogate markers for axonal injury, degeneration and loss. J Neurol Sci 2004;233:183–98
38. Ling EA, Paterson JA, Privat A, et al. Investigation of glial cells in semithin sections. I. Identification of glial cells in the brain of young rats. J Comp Neurol 1973;149:43–72
39. Ling EA, Leblond CP. Investigation of glial cell in semithin section. II. Variation with age in the numbers of various glial cell types in rat cortex and corpus callosum. J Comp Neurol 1973;149:73–82
40. Peters A, Palay SL, Webster HW. *The Fine Structure of the Nervous System*. 3rd ed. New York, NY: Oxford University Press, 1991
41. Rozen S, Skalesky HJ. Primer 3 on the WWW for general users and for biologist programmers. In: Krawetz S, Misener S, eds. *Bioinformatics Methods and Protocols: Methods in Molecular Biology*. Totowa, NJ: Humana Press, 2000:365–86
42. Pfaffl MW. Quantification strategies in real-time PCR. In: Bustin SA, ed. *A–Z of Quantitative PCR*. La Jolla, CA: International University Line, 2004:87–112
43. Butts BD, Houde C, Mehmet H. Maturation-dependent sensitivity of oligodendrocyte lineage cells to apoptosis: Implications for normal development and disease. Cell Death Differ 2008;15:1178–86
44. Du Y, Dreyfus CF. Oligodendrocytes as providers of growth factors. J Neurosci Res 2002;68:647–54
45. Nave K-M. Myelination and the trophic support of long axons. Nat Rev Neurosci 2010;11:275–85
46. Soldán MM, Pirko I. Biogenesis and significance of central nervous system myelin. Semin Neurol 2012;32:9–14
47. Wilkins A, Majed H, Layfield R, et al. Oligodendrocytes promote neuronal survival and axonal length by distinct intracellular mechanisms: A novel role for oligodendrocyte-derived glial cell line–derived neurotrophic factor. J Neurosci 2003;23:4967–74
48. Staugaitis SM, Trapp BD. NG2-positive glia in the human central nervous system. Neuron Glia Biol 2009;5:35–44
49. Ando S, Tanaka Y, Toyoda Y, et al. Turnover of myelin lipids in aging brain. Neurochem Res 2003;28:5–13
50. Winterstein C, Trotter J, Krämer-Albers E-M. Distinct endocytic recycling of myelin proteins promotes oligodendroglia remodeling. J Cell Sci 2008; 121:834–42
51. Bray GM, Duncan ID, Griffiths IR. ''Shaking pups'': A disorder of central myelination in the spaniel dogs. IV. Freeze-fracture electron microscopy studies of axons, oligodendrocytes and astrocytes in the spinal cord white matter. Neuropathol Appl Neurobiol 1983;9:369–78
52. Graham RK, Ehrnhoefer DE, Hayden MR. Caspase-6 and neurodegeneration. Trends Neurosci 2011;34:646–56
53. Parente MK, Rozen R, Cearley CN, et al. Dysregulation of gene expression in a lysosomal storage disease varies between brain regions implicating unexpected mechanisms of neuropathology. PLoS One 2012; 7:e32419

